Simultaneous detection of SARS-CoV-2 RNA and host antibodies enabled by a multiplexed electrochemical sensor platform

Helena de Puig[1, 2 #], Sanjay Sharma Timilsina[1 #], Joshua Rainbow[1, 3 #], Pawan Jolly[1 #], Devora Najjar[1, 2, 4], Nolan Durr[1], Galit Alter[5], Jonathan Z. Li[6], Xu G. Yu[5, 6], David R. Walt[1, 7, 8], Pedro Estrela[3], James J. Collins[1, 2, 9], Donald E. Ingber[1, 7, 10, 11 *]

[1]Wyss Institute for Biologically Inspired Engineering, Harvard University, Boston, MA 02115, USA
[2]Institute for Medical Engineering and Science, Department of Biological Engineering, Massachusetts Institute of Technology, Cambridge, MA 02139, USA
[3]Centre for Biosensors, Bioelectronics and Biodevices (C3Bio) and Department of Electronic and Electrical Engineering, University of Bath, Bath BA2 7AY, UK
[4]MIT Media Lab, Massachusetts Institute of Technology, Cambridge, MA 02139, USA
[5]Ragon Institute of MGH, MIT, and Harvard, Cambridge, MA 02139, USA.
[6]Division of Infectious Diseases, Brigham and Women's Hospital, Boston, MA 02115, USA
[7]Harvard Medical School, Boston, MA 02115, USA
[8]Department of Pathology, Brigham and Women's Hospital, Boston, MA 02115, USA
[9]Infectious Disease and Microbiome Program, Broad Institute of MIT and Harvard, Cambridge, MA 02142, USA
[10]Vascular Biology Program and Department of Surgery, Boston Children's Hospital, Boston, MA 02115, USA
[11]Harvard John A. Paulson School of Engineering and Applied Sciences, Harvard University, Boston, MA 02115, USA

* Address all correspondence to: Donald E. Ingber, MD, PhD, Wyss Institute at Harvard University, CLSB5, 3 Blackfan Circle, Boston MA 02115, USA (phone: 617-432-7044, fax: 617-432-7828; e-mail: don.ingber@wyss.harvard.edu
# These authors contributed equally

Keywords: CRISPR, diagnostic, serology, antibody, electrochemical sensor, COVID-19, saliva, SARS-CoV-2, point-of-care, antifouling.

Abstract

There continues to be a great need for rapid, accurate, and cost-effective point-of-care devices that can diagnose the presence of SARS-CoV-2 virus and development of IgG and IgM antibody responses in early and late stages of COVID-19 disease. Here, we describe a versatile multiplexed electrochemical (EC) sensor platform modified with an antifouling nanocomposite coating that enables single-molecule CRISPR/Cas-based molecular detection of SARS-CoV-2 viral RNA with on-chip signal validation as well as multiplexed serological detection of antibodies against three SARS-CoV-2 viral antigens. The CRISPR-based EC platform achieved 100% accuracy for detection of viral RNA and showed an excellent correlation with RT-qPCR using 30 clinical saliva samples. The serology EC platform obtained 100% sensitivity and 100% specificity for anti-SARS-CoV-2 IgG, as well as 94% specificity and 82% sensitivity for anti-SARS-CoV-2 IgM with 112 clinical plasma samples. These data demonstrate that integration of CRISPR-based RNA detection and serological assays with antifouling nanocomposite-based EC sensors enables performance as good or better than traditional laboratory-based techniques.

The COVID-19 pandemic has made it evident that cost-effective diagnostics for SARS-CoV-2 RNA and viral antigen-targeted immunoglobulins generated by the host in response to infection are urgently needed to improve patient care and prevent disease transmission. This type of multifunctional detection platform would be particularly useful for diagnosis of both acute and convalescent infections, as well as for assessing patient immunization status following vaccination. The clinical timeline of SARS-CoV-2 infection consists of an acute phase, when viral RNA is detectable in clinical samples, such as saliva or nasopharyngeal swabs, followed by a convalescent phase when serology biomarkers, such as IgG and IgM antibodies, are present in blood. Therefore, analysis of these different biomarkers in clinical samples from the sample patient at the same time and as the disease progresses could provide more accurate results for disease management. Molecular (nucleic acid) diagnostics that detect the presence of viral RNA are key to detecting the virus during the first 5 days of infection, with a viral load peak around day 4 (Supplementary Fig. S1)[1,2,3]. Following the first few days of infection, the host produces IgM, IgA, and IgG antibodies in a process known as seroconversion. These antibodies often become stable after the first 6 days of seroconversion and their titer remains stable over months[4,5] .The presence of different antibody types varies during infection[6] and correlates with disease severity[7,8]. In particular, extensive cohort studies in hospitalized patients show that IgG antibodies against the S protein are more specific[9] and correlate with virus neutralization[7], while antibodies against the N protein appear earlier during infection[10]. Therefore, serological assays that detect the host's antibodies developed after an infection can widen the testing window for SARS-CoV-2 beyond the molecular diagnostic timeframe and provide insights into the patient's progression and more accurate estimates of when the patient was initially infected. They also may be used to ensure the effectiveness of vaccination responses, and whether or not they are maintained over time. For example, SARS-CoV-2 vaccine efficacy trials have highlighted a direct correlation between the titer of antibodies targeting the Receptor Binding Domain (RBD) of the Spike protein, the neutralizing antibody titer, and vaccine efficacy[11]. Thus, the development of serological assays targeted to individual SARS-CoV-2 viral antigens could have important implications for predicting the efficacy vaccines and estimating the need for boosters.

Molecular diagnostics, on the other hand, commonly involve use of RT-qPCR, which requires rigorous sample preparation and temperature control, cold storage of reagents, expensive instrumentation (requiring routine maintenance), and trained personnel to run the tests. During the last few years, powerful diagnostic techniques that capitalize on Clustered Regularly Interspaced Short Palindromic Repeats (CRISPR) and associated programmable endonucleases have gained significant interest, due in part to their high specificity, programmability, and capacity to work at physiological conditions[12-16]. CRISPR-based diagnostics capitalize on endonucleases, such as Cas12a, which has a specific cleavage activity towards double-stranded DNA (dsDNA) fragments matching its guide RNA (gRNA) sequence. Once the Cas12a-gRNA complex binds to its dsDNA target, it activates and subsequently engages in indiscriminate collateral hydrolysis of nearby single-stranded DNA (ssDNA)[17,18]. Electrochemical (EC) methods of CRISPR-based nucleic acid detection typically combine nucleic acid probes conjugated on an electrode with CRISPR-Cas effectors, and have detection limits in the picomolar-femtomolar (10^{-12}-10^{-15}) range[19,20]. Unfortunately, that limit of detection is inadequate for diagnosing SARS-CoV-2 clinical samples, which require ultrasensitive RNA detection at the attomolar (10^{-18}) scale. To overcome this limitation, we previously integrated an isothermal amplification technique — loop-mediated isothermal amplification (LAMP) — before the Cas12a detection, which can improve the sensitivity of fluorescent CRISPR-based assays by orders of magnitude[12-14,16,21].

Combining serological and nucleic acid diagnostics improves the overall accuracy of SARS-CoV-2 diagnosis[22] and provides qualitative data on the patient's disease severity and state of progression; however, this is usually only possible in a hospital setting. EC biosensors that integrate biological probe molecules offer a particularly promising solution to achieve similar ultra-sensitive, selective, multiplexed, quantitative, and cost-effective detection of both nucleic acids and proteins, while enabling this to be carried out in a point-of-care (POC) setting. Moreover, EC sensors have the potential to interface with electronic medical records, integrated cloud systems, and telemedicine. But EC diagnostic platforms have only been used to detect either nucleic acid or proteins in the past[20,23]. Thus, there is a need for a potentially portable diagnostic platform that is versatile enough to detect both nucleic acids and proteins simultaneously, and particularly for detection of SARS-CoV-2 RNA and host antibodies directed against the virus.

While EC sensors remain the workhorse of choice for such versatile biosensing devices, a key challenge that has prevented their widespread use and market penetration is biofouling, the accumulation of unwanted material present in complex biological fluids on their surface. Biofouling can lead to degradation of deposited surface chemistries and a reduction in the observable signal change upon target molecule binding, leading to a loss of sensitivity and specificity[24]. To prevent biofouling, we previously reported a conducting nanocomposite coating composed of glutaraldehyde (GA) cross-linked denatured bovine serum albumin (BSA) doped with conductive reduced graphene oxide (rGOx), which provides ultra-high specificity and allows functionalization with surface ligands[25,26]. EC sensors modified with this antifouling coating can be used to detect different antigens in a multiplexed fashion with minimal cross-reactivity[27]. Thus, in the present study, we set out to explore whether this multiplexed EC sensor platform could be used in combination with CRISPR/cas molecular diagnostics to detect both SARS-CoV-2 viral RNA and monitor immune responses in clinical samples.

Results

Optimization of a CRISPR-based sensor for SARS-CoV-2 viral RNA

The CRISPR-Cas RNA detection experiments reported here capitalize on Cas12a from *Lachnospiraceae* bacterium ND2006, which has specific cleavage activity towards dsDNA fragments matching its guide RNA (gRNA) sequence. Upon target binding, activated Cas12a-gRNA engages in collateral cleavage of nearby single-stranded DNA (ssDNA)[17,18] which can be read optically as an increase in fluorescence due to the hydrolysis of a fluorophore-quencher labeled ssDNA reporter. LAMP primers[28-32] and Cas12a-gRNAs were evaluated from a range of conserved regions in the SARS-CoV-2 genome to determine the most sensitive combinations using commercially available, synthetic full-length SARS-CoV-2 genomic RNA. The ORF1a assay, which targets a highly conserved region in the SARS-CoV-2 viral genome, had a limit of detection (LOD) of 2.3 viral RNA copies/μL with a reaction time of 50 min (Supplementary Table S1, Fig. S2, Fig. S3). This LOD is comparable to high-performance SARS-CoV-2 RT-qPCR assays[33], with half the time to result.

To confirm that the assay was able to detect SARS-CoV-2 active virus, the ORF1a assay primers and guide RNA were further validated using 11 SARS-CoV-2 RT-qPCR negative patient saliva samples and 19 SARS-CoV-2 RT-qPCR positive saliva samples with a range of cycle threshold (C_T) values (Supplementary Fig. S4). Briefly, total RNA was extracted from saliva using a commercially available QIAamp viral RNA mini kit (Qiagen), which serves the dual function of purifying the viral RNA and both inactivating and lysing viral particles in approximately 15 min. After that, extracted RNA was tested in our LAMP/Cas12a fluorescent assays, which showed an excellent correlation with RT-qPCR (Supplementary Fig. S4, Supplementary Table S2).

Integration of the CRISPR-based molecular diagnostic in the EC sensor platform

To integrate the CRISPR-based molecular assay into the EC sensor platform, we designed a biotinylated ssDNA reporter probe (RP) that partially hybridized to peptide nucleic acid (PNA) capture probes which were immobilized on the surface of the antifouling composite that was precoated on the gold electrodes, as previously described[25](Fig. 1a-c), and four electrodes were multiplexed in each chip. For internal chip validation, three working electrodes were functionalized with the amine-terminated capture PNA probe, and one electrode was modified with 0.1 mg/mL BSA as a negative control. Functionalized EC biosensors were incubated with samples containing the LAMP/Cas12a mix, and the biotinylated ssDNA RP as described in methods (Fig. 1a). In the presence of SARS-CoV-2 target RNA, Cas12a collaterally cleaved the biotinylated ssDNA reporter, leading to a reduction of binding of poly-horseradish peroxidase (HRP)-streptavidin and thus, a reduction in the precipitation of tetramethylbenzidine (TMB), which deposits locally on the surface of the electrode[25] (Fig. 1b). Reduced precipitation of TMB was recorded as peak current, which was measured using cyclic voltammetry (CV) by sweeping the voltage between -0.5 and 0.5 V (Fig. 1c). As a result, the signal obtained from the EC platform demonstrated an inversely proportional relationship with target concentrations.

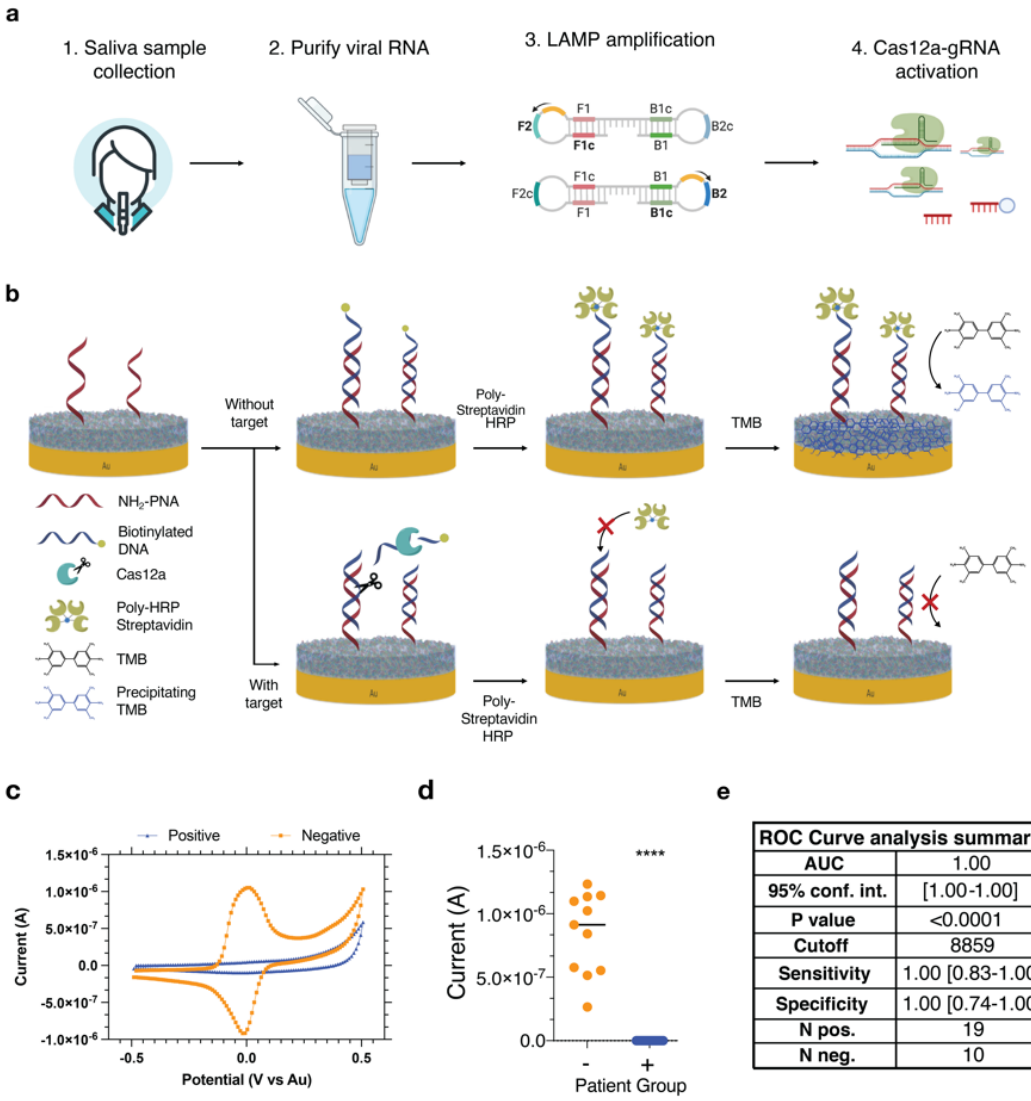

ROC Curve analysis summary	
AUC	1.00
95% conf. int.	[1.00-1.00]
P value	<0.0001
Cutoff	8859
Sensitivity	1.00 [0.83-1.00]
Specificity	1.00 [0.74-1.00]
N pos.	19
N neg.	10

Fig. 1. Schematic of the CRISPR electrochemical assays and assay performance using clinical samples. (a) Collection of patient saliva samples, sample preparation, amplification, and collateral cleavage by Cas12a enzyme. (b) Schematic illustrating the surface chemistry of the electrochemical assay. Without viral RNA present, poly-HRP streptavidin binds to the PNA/biotin-DNA duplex and consequently precipitates TMB resulting in an increase in current. In contrast, in the presence of viral target RNA, the biotinylated reporter ssDNA is hydrolyzed, cleaving the biotin group. Consequently, poly-HRP streptavidin does not bind to the surface of the chips, resulting in no TMB precipitation and no increase in current. (c) Cyclic voltammogram showing the typical current peak signal achieved after incubation of samples from both SARS-CoV-2 negative (blue) and positive (orange) clinical samples. (d) Clinical samples that contained SARS-CoV-2 viral RNA (+, blue) had low signals in our device and were clearly distinguishable from the high signals obtained for samples that did not contain viral RNA (-, orange). Student's t-test p value <0.001 (***). (e) Summary table listing the numerical values of the receiver operating characteristic (ROC) curve analysis of the patient sample data collected for the SARS CoV-2 assay. The table shows a summary of the results from 19 RT-qPCR confirmed positive and 10 negative human saliva samples. AUC: area under the curve; 95% conf. Int.: 95% confidence interval; Sens: sensitivity; Spec.: specificity; N pos.: number of RT-qPCR SARS-CoV-2 positive samples; N neg.: number of RT-qPCR SARS-CoV-2 negative clinical samples.

The binding efficiency of the PNA-based CRISPR-EC sensor platform was optimized by varying the concentration and incubation time of RP to obtain a rapid high signal-to-noise ratio (Supplementary Fig. S5 and S6). Among all the concentrations tested, 1nM RP and 5 min incubation produced a high signal with no background. We then measured the LOD of the EC-CRISPR platform using serial dilutions of full-length SARS-CoV-2 genomic RNA in water. LAMP was used to amplify the viral RNA, and the resulting reaction mixture was then added to Cas12a-gRNA complex and EC ssDNA RP. The specific binding of Cas12a-gRNA to the target dsDNA resulted in enzyme activation and cleaved the biotinylated ssDNA reporter probe. Cleaved biotinylated RP does not bind to the PNA on the electrodes, resulting in a lower signal from the EC platform. Interestingly, the CRISPR-EC sensor platform gave a single molecule LOD of 0.8 cp/μL, which was nearly four times more sensitive than the initial fluorescence-based assays used to validate the primer and guide pairs (Supplementary Table S1, Figs. S3 and S7).

To determine the potential clinical value of the optimized CRISPR-EC sensor platform, RNA was extracted from 19 saliva samples from patients that were positive for SARS-CoV-2 based on RT-qPCR with a range of CT values and 11 RT-qPCR negative clinical saliva samples (Supplementary Fig. S8). The current measured in the form of the output signal from the electrodes was clearly distinguishable (p-value <0.0001) when comparing the SARS-CoV-2 positive and negative samples (Fig. 1d). In addition, ROC curve analysis demonstrated an impressive correlation with RT-qPCR and CRISPR-based fluorescent detection, with 100% accuracy, and AUC=1 (Fig. 1e).

Multiplexed serology EC platform

Multiplexed assays that diagnose disease by combining serology markers and viral RNA lead to higher specificity and sensitivity against diseases, including SARS-CoV-2[34]. The primary antigens that elicit antibodies during coronavirus infection are the viral nucleocapsid (N) and Spike (S) proteins[9]. The N protein is the most abundant viral protein, and it is highly conserved among the coronavirus family[35]. While the S protein is less conserved than N, it is highly immunogenic and its Receptor Binding Domain (RBD) is key for viral entry to cells[36]. Several studies show that IgG antibodies targeting the S protein are more specific for SARS-CoV-2, while those targeting the N protein may be more sensitive, particularly in the early phase of infection[6]. Therefore, to maximize our assay's accuracy for both early and late infections, we fabricated a multiplexed serology assay capable of measuring antibodies against S1-RBD, S1, and N proteins.

An Enzyme-Linked Immunosorbent Assay (ELISA) was used to optimize the reagents prior to building the multiplexed serology EC sensor platform (Supplementary Figs. S9-S13). The best performing capture antigens were Spike S1 (S1, SinoBiological, China, no. 40591-V08H), Nucleocapsid (N, RayBiotech, US, no. 130-10760), and Spike-RBD (S1-RBD, The Native Antigen Company, UK, no. REC31849). The best performing detection antibodies were biotinylated goat anti-human IgG (109-006-170), HRP conjugated rabbit anti-human IgM (109-4107), and HRP conjugated goat anti-human IgA (109-005-011). We validated the ELISA accuracy with 58 SARS-CoV-2 plasma samples from patients with a prior positive SARS-CoV-2 RT-qPCR result and with 54 SARS-CoV-2 negative samples. Out of the 54 negative SARS-CoV-2 samples, 22 were collected before the onset of the SARS-CoV-2 pandemic. The ROC curve analysis of the ELISA results

showed areas under the curve (AUC) for IgG, IgM and IgA between 0.68-0.89 (Supplementary Figs. S11-S13).

We next used the optimized reagents to develop multiplexed EC sensors to measure the humoral response against SARS-CoV-2 in clinical samples. An advantage of using EC biosensors to monitor immune response is that the miniaturized electrodes only require 1.5 μL of undiluted plasma, which can easily be obtained by a finger prick. Moreover, the antifouling properties of the BSA/rGOx/GA surfaces on the EC sensor chips lead to higher sensitivity and specificity of our EC assays compared to ELISAs due to their ultra-low EC noise. We built BSA/rGOx/GA coated sensors where each electrode was individually functionalized with S1 (electrode 1), S1-RBD (electrode 2), N (electrode 3), or BSA as an on-chip negative control (electrode 4) to perform a multi-antigen sandwich EC ELISA (Fig. 2a). We used an affinity-based sandwich strategy as in the EC sensor platform so that when SARS-CoV-2 antibodies were present, they bound to both the surface antigen and secondary antibody, leading to a higher EC signal. Each immunoglobulin isotype (IgG, IgM, IgA) was detected individually with different EC chips coated with ligands for the 3 different viral antigens and BSA control. Fig. 2b-e shows typical CV results obtained with the multiplexed EC chips for detection of anti-SARS-CoV-2 IgG and IgM using SARS-CoV-2 positive and negative clinical samples. The assay conditions of the serology EC assays were optimized to obtain the highest signal-to-noise ratios in high- and low- antibody titer clinical samples. This was accomplished by optimizing plasma dilutions, sample incubation times, and TMB precipitation times (Supplementary Figs. S14 - S16). We found that optimal conditions for the assay included a 30 min sample incubation at a 1:9 plasma dilution with a 3 min TMB precipitation time, which resulted in high sensitivity and specificity for detection of SARS-CoV-2 antibodies in clinical plasma samples (Supplementary Fig. S15 c).

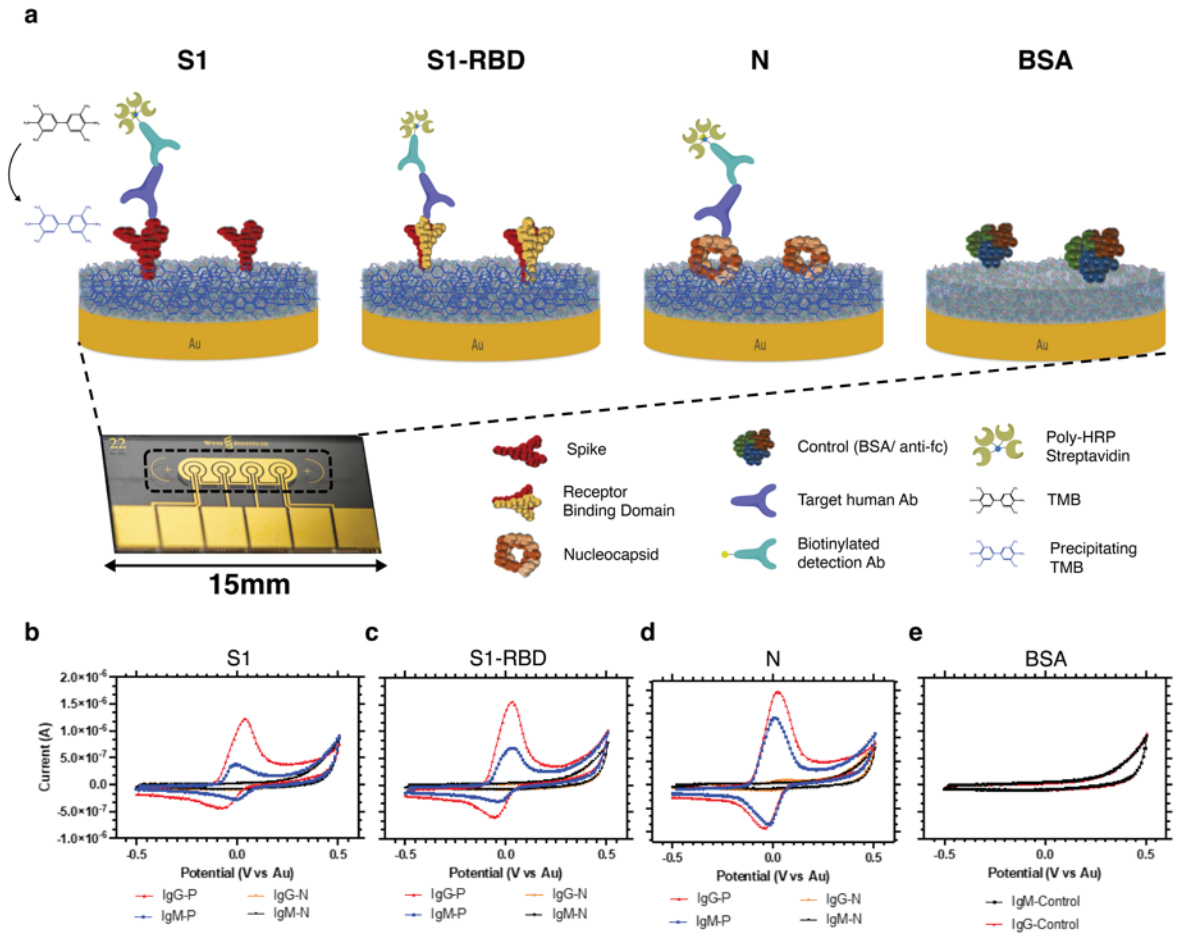

Fig. 2: Schematic and representative raw cyclic voltammetry data of the multiplexed serology assay. (a) Schematic illustrating the multiplexed electrochemical serological assay to assess host antibody responses on electrodes functionalized with SARS-CoV-2 antigens. Host antibodies bind to the SARS-CoV-2 antigens immobilized on the chips. Subsequently, biotinylated anti-human IgG secondary antibodies bind, followed by poly HRP-streptavidin binding and TMB precipitation on the chips. (b-e) Typical cyclic voltammograms for the four different electrodes that target host antibodies against (b) Spike 1 subunit (S1), (c) Spike 1-receptor binding domain (S1-RBD), (d) nucleocapsid (N), and (e) BSA negative control with positive (red, blue) and negative (orange and black) samples for IgG and IgM, respectively.

We then evaluated the accuracy of the EC serology platform using plasma samples from patients with a prior SARS-CoV-2 RT-qPCR positive result. ROC curve analysis was done using 58 SARS-CoV-2 positive plasma samples and 54 SARS-CoV-2 negative samples. Out of the 54 SARS-CoV-2 negative samples, 22 were pre-pandemic healthy controls. Overall, the AUC for anti-SARS-CoV-2 IgG (Fig. 3a,c) was higher than IgM (Fig. 3b,c), whereas IgA's AUC was low (between 0.57-0.78) and did not add diagnostic value (Supplementary Fig. S17). The specificity of all individual sensors modified with either S1, N or RBD was over 95% for both IgG and IgM. However, the sensitivity was overall lower for IgM assays as compared to IgG. The lower performance in IgM assays correlated with prior ELISA results and was likely attributed to the fluctuation in IgM concentrations during the course of the disease and late collection of the clinical samples[37,38].

a

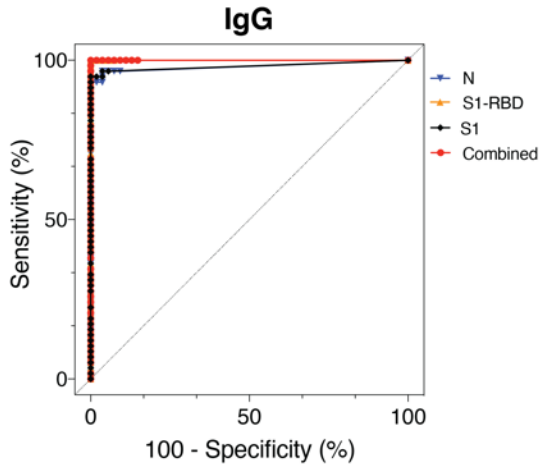

b

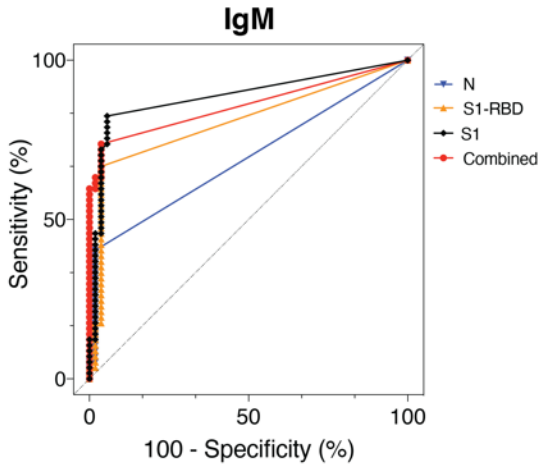

c

	IgG				IgM			
	S1	S1-RBD	N	Combined	S1	S1-RBD	N	Combined
AUC	0.98	1.00	0.98	1.00	0.70	0.86	0.80	0.89
95% conf. int.	[0.95-1.00]	[1.00-1.00]	[0.95-1.00]	[1.00-1.00]	[0.59-0.79]	[0.79-0.93]	[0.72-0.89]	[0.82-0.95]
P value	<0.0001	<0.0001	<0.0001	<0.0001	0.0006	<0.0001	<0.0001	<0.0001
Cutoff	>1.9e-7	>1.7e-7	>3.1e-8	>2.4e-7	>9.3e-9	>2.1e-9	>5.3e-9	>5.3e-9
Sens.	0.95 [0.83-0.97]	1.00 [0.94-1.00]	0.95 [0.86-0.98]	1.00 [0.94-1.00]	0.40 [0.29-0.53]	0.73 [0.61-0.83]	0.67 [0.54-0.78]	0.83 [0.71-0.90]
Spec.	1 [0.93-1.00]	1.00 [0.93-1.00]	1 [0.93-1.00]	1.00 [0.93-1.00]	0.98 [0.90-1.00]	0.96 [0.88-0.99]	0.96 [0.87-0.99]	0.95 [0.85-0.99]
N pos.	54	54	54	54	54	54	54	54
N neg.	58	58	58	58	57	57	57	57

Fig. 3. Multiplexed electrochemical assays accurately detect host antibodies against SARS-CoV-2 in clinical samples. (a) ROC curves generated from the patient sample data obtained for the IgM electrochemical serology assay. (b) ROC curves generated from the patient samples data obtained for the IgG electrochemical serology assay. (c) Table listing the numerical values of the sensitivity and specificity results. AUC: area under the curve; 95% conf. Int.: 95% confidence interval; Sens: sensitivity; Spec.: specificity; N pos.: number of gold standard SARS-CoV-2 positive samples; N neg.: number of gold standard SARS-CoV-2 negative clinical samples.

Further analysis of the multiplexed assay's ROC curves revealed that S1-RBD was the most accurate capture probe (AUC=1 for IgG; AUC=0.86 for IgM), followed by N and S1 (Fig. 3c). Adding the output results from the three antigens as a multiplexed readout (Combined, Fig. 3) also led to a slight increase in accuracy (AUC=1 for IgG; AUC=0.89 for IgM). As the combined EC IgG assay had an excellent correlation with prior SARS-CoV-2 infection and was 100% accurate (100% sensitivity and specificity), we used this for subsequent multiplexed experiments in single chips. The EC sensor-based serology platform was also more accurate in detecting samples from patients with prior SARS-CoV-2 infection than the ELISA. The high specificity of the EC sensor platform may be attributed to the low non-specific binding on our nanocomposite-coated EC electrodes. The BSA/rGOx/GA antifouling coating also contributed to the high sensitivity we observed because it allowed us to probe in highly concentrated plasma, increasing the availability of antibodies that would otherwise be too dilute to detect.

Proof-of-concept for multiplexed CRISPR-based assay and serology

To explore the potential for multiplexing CRISPR-based molecular diagnostics and serology assays for COVID-19, we modified each of the four electrodes with one the three antigens: S1, N, S1-RBD, or PNA alone (Fig. 4a), with the goal of carrying out simultaneous multiplexed detection of viral RNA and serology markers in a single chip because this could result in increasing the sensitivity and specificity of SARS-CoV-2 detection[34]. Saliva is an excellent source of both viral RNA as well as host antibodies (IgG, IgM, IgA) in SARS-CoV-2 patients[39], and hence, it is an ideal sample for a multiplexed assay for viral RNA and serology. Because saliva of SARS-CoV-2 infected patients is highly contagious, it had to be heat-inactivated before testing it in our multiplexed platform; however, saliva antibodies are denatured by high temperatures[40]. Therefore, in order to demonstrate the performance of our multiplexed RNA and antibody diagnostic platform, we heat-inactivated saliva from SARS-CoV-2 infected patients (or negative controls) and then spiked the saliva with human plasma from control or SARS-CoV-2 patients at 1:20 to simulate the ratio of IgG present in saliva compared to human serum (Supplementary Fig. S18).

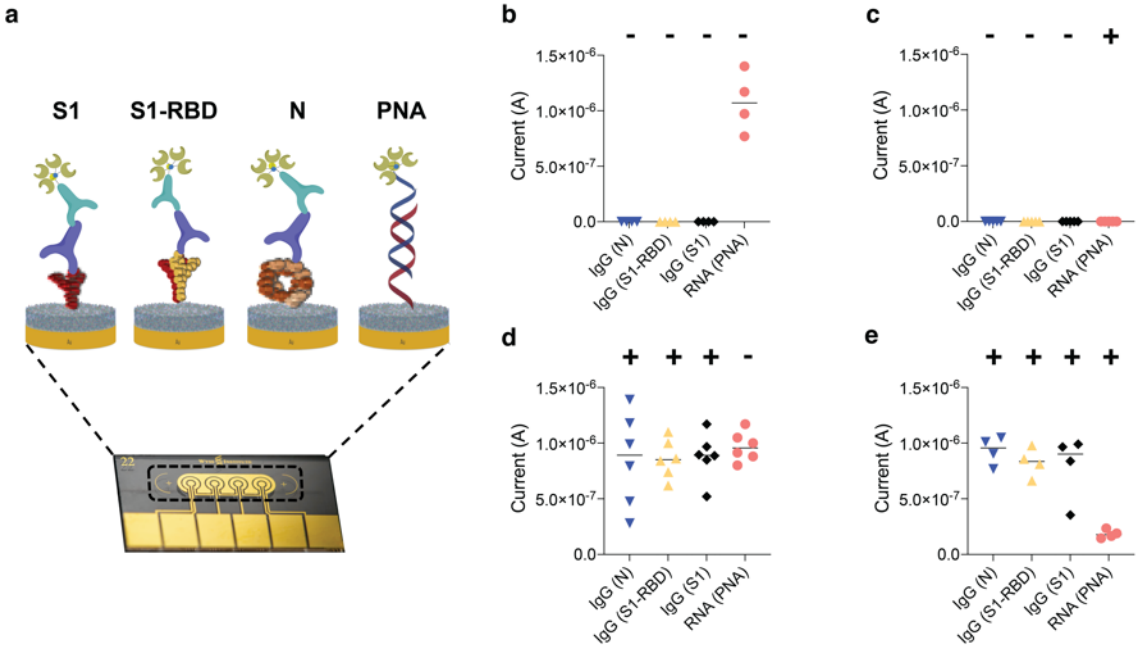

Fig. 4. Electrochemical platforms can be used for simultaneous detection of SARS-CoV-2 viral RNA and host antibodies against the virus. (a) Schematic of the multiplexed chip surface conjugated with SARS-CoV-2 antigens: Spike (S1), S1-Receptor binding domain (S1-RBD), and Nucleocapsid (N); as well as peptide nucleic acid (PNA) for the detection of SARS-CoV-2 viral RNA. (b-e) Current (A) electrochemical readout for clinical samples that contain different host antibody and viral RNA combinations: (b) Clinical samples negative for both serology and viral RNA. (c) Clinical samples with negative host antibody levels and positive for viral RNA. (d) Clinical samples that contain host antibodies against SARS-CoV-2 but are negative for viral RNA, and (e) clinical samples with both positive host antibodies and viral RNA. The RNA signal significantly decreases (P value = 0.0006, Student's t test) when comparing IgG-positive and viral RNA-positive (e) and RNA negative samples (b and d).

A two-step assay using the same functionalized chip was performed as follows: plasma-spiked saliva was split into two volumes: 15μl was first incubated on the chip for multiplexed serological detection of the host's anti-SARS-CoV-2 antibodies, and 400μl were used for RNA extraction followed by CRISPR-based detection on the same chip. After that, we simultaneously measured the SARS-CoV-2 viral RNA and host antibodies on-chip with the electrochemical readout of precipitating TMB. We validated the assay performance by testing the four possible combinations of serology and RNA-positive and negative clinical samples (Fig. 4b-e). Clinical IgG negative samples showed no electrochemical signals for the N, S1 and S1-RBD antigen-conjugated electrodes (Fig. 4b, c), whereas clinical samples from patients exposed to SARS-CoV-2 had high IgG loads in all three antigen test areas (Fig. 4 d, e). Moreover, we measured high currents in the PNA conjugated electrodes for all the clinical samples that were negative for SARS-CoV-2 viral RNA (Fig. 4b, d, red circles), as well as low currents in the PNA electrodes for SARS-CoV-2 RT-qPCR RNA positive samples (Fig. 4 c, e, red circles). A low background current ($1.8 \times 10^{-7} \pm 3.7 \times 10^{-8}$) was measured on the PNA electrodes on the chips that were incubated with SARS-CoV-2 serology positive and RNA positive samples (Fig. 4e), potentially due to either interaction of IgG with PNA probes or precipitated TMB background contaminations from the IgG-positive electrodes to the PNA electrode. Nevertheless, the low background signal in the PNA electrodes that were incubated with RNA RT-qPCR and IgG positive samples was clearly distinguishable (student's t-test $p<0.0001$) from the signal obtained on the PNA electrodes for SARS-CoV-2 viral RNA negative samples (Fig. 4b, d, $1.0 \times 10^{-6} \pm 1.9 \times 10^{-7}$). Taken together, the results show excellent multiplexing capacity for SARS-CoV-2 viral RNA and host antibodies on the chips with 100% correlation in specificity and sensitivity. Thus, this is the first report that demonstrates proof-of-concept for using a single EC sensor chip with multiple electrodes for the multiplexed detection of antibodies and RNA for SARS-CoV-2.

Discussion

Molecular diagnostics for detection of pathogen RNA and serological assays for assessment of host antibody responses are complementary tools that provide critical information to respond to epidemics and manage patient care and risks. Molecular diagnostics for SARS-CoV-2 RNA are indicators of viral shedding during the infectious phase of the disease; however, they can often still detect the presence of viral RNA long after the infectious phase has subsided. The sensitivity of molecular diagnostics also varies considerably over the course of the disease, sample type, virus variants, and infection severity[41-46]. On the other hand, serological assays detect prior viral infections or productive vaccinations because they measure the antibodies that the host produces as a defense against pathogens. As antibodies are long-lived in a patient's blood after infection, combining molecular diagnostics with serological assays improves the probability of detecting present and past infections. This approach also can be used to assess patient responses to vaccination[11] and to help determine when boosters might be required. Unfortunately, efficacious and inexpensive dual serology and molecular SARS-CoV-2 assays are still unavailable despite urgent needs.

In the present study, we described an ultra-sensitive, highly specific, and rapid multiplexed EC platform, which can detect both the SARS-CoV-2 viral RNA and antibodies from clinical samples.

Because of its customizable surface chemistry with different probes, these EC sensors enable the detection of different targets such as nucleic acids and proteins. Additionally, the BSA/rGOx/GA-based surface chemistry allows for high conductivity and low nonspecific binding leading to ultra-low electrochemical background, thereby increasing the sensitivity and selectivity[27,28]; the coating materials and methods are also simple and inexpensive[27]. Importantly, by leveraging this nanocomposite-coated EC sensor technology, we were able to construct a multiplexed EC sensor that simultaneously detects viral RNA and different antibody isotypes (IgG/IgM) against relevant viral structural proteins (S1-RBD, S1, and N), allowing for a more robust understanding of the humoral response in patients.

Multiplexed serology assays are increasingly relevant due to the current rate of vaccine rollout. For example, SARS-CoV-2 vaccines in the market induce antibody production against SARS-CoV-2 S protein, and vaccinated individuals without infection by SARS-CoV-2 are expected to develop measurable antibodies against the S but not the N protein[47]. Therefore, multiplexed serology assays that target antibodies against several viral antigens might become key for seroprevalence studies to estimate the proportion of people in a population that have been infected, including asymptomatic infection, and/or immunized with vaccines. This information is key to estimate herd immunity and vaccine efficacy[11], which is critical for the decision to reopen economies[48,49].

The vast majority of serology assays approved by the Food and Drug Administration (FDA) and Conformité Européene (CE) mark are not multiplexed and target antibodies developed against a few viral surface proteins. In contrast, our multiplexed EC platform has accuracies similar or better than traditional serology assays (e.g., ELISA), with a faster time to readout (30 min) and very low sample volume requirements (1.5 μL), which can be easily obtained by finger prick collection[50,51]. We validated the serology platform with 112 clinical plasma samples and showed a higher accuracy of 100% (100% sensitivity and 100% specificity) for IgG detection and a 0.89 AUC (95% specificity and 83% sensitivity) for IgM compared to traditional ELISA. We also found that multiplexing results from different viral antigens led to increased sensitivity in the assays. Among the three antigens tested, S1-RBD was the most accurate in detecting IgG and IgM in clinical samples, which can be explained by the fact that the RBD domain is a highly immunogenic epitope for development of neutralizing antibodies during the humoral response to SARS-CoV-2[52].

We further demonstrated the versatility of our EC sensor platform for nucleic acid detection by building molecular assays that target SARS-CoV-2 viral RNA in saliva. Our molecular assay builds off of CRISPR-based diagnostics that combine isothermal nucleic acid amplification together with CRISPR-Cas enzymes, such as SHERLOCK[13,14] or DETECTR[12]. CRISPR/Cas effectors have revolutionized nucleic acid diagnostics due to their sensitivity, specificity, multiplexing capacity, ease of use, low cost, and ability to detect many nucleic acid sequences of interest[21]. CRISPR diagnostics have been stabilized in a freeze-dried format for cold-chain free deployment[53,54], opening the possibility to shelf-stable storage of multiplexed CRISPR diagnostic chips used for detection[15]. Moreover, CRISPR effectors have evolved to achieve specific recognition of nucleic acids at physiological temperatures, thus widening their application in POC diagnostics. Other CRISPR-Cas diagnostics for SARS-CoV-2 have been described[55-57], but are usually limited to fluorescence and lateral flow readouts.

The integrated CRISPR-based EC sensor platform described here demonstrated excellent performance compared to RT-qPCR using saliva samples. Our study was limited by the small set of clinical COVID-19 saliva samples available due both to the difficulty in acquiring saliva through biorepositories that do not routinely collect this sample type, as well as the difficultly in procuring these samples within the context of a proof-of-concept exploratory study. However, the fact that we could obtain 100% accuracy with clinical samples characterized by a wide range of viral loads strongly suggests that our CRISPR-based EC sensor platform could become a faster, simpler, and cheaper non-invasive strategy compared to RT-qPCR and traditional fluorescent diagnostics. Additionally, saliva is an excellent alternative to nasopharyngeal swabs and nasal swabs for SARS-CoV-2 diagnosis, as it is easy to collect, and does not require collection equipment other than a simple container. Even though saliva is not a standard sample type for SARS-CoV-2 diagnosis, the viral load of SARS-CoV-2 in saliva has been shown to be similar to nasopharyngeal swabs and to be present for a greater number of days[58,59]. Moreover, saliva is an ideal sample material for combined SARS-CoV-2 serology and viral RNA detection because it also contains measurable antibody titers[60]. Therefore, in this report, we demonstrated the versatility of our platform by using the same chip for simultaneous detection of both RNA and IgG in clinical saliva samples. Future work for our device includes fully integrating the various components into a device platform for miniaturized and POC testing and optimizing the sensors to perform using saliva for both serology and viral RNA detection.

Methods

Preparation of chips

Gold chips were custom manufactured by Telic Company using a standard photolithography process with deposition of 15 nm of chromium and 100 nm of gold on a glass wafer. The area of electrodes was controlled by depositing a layer of 2 μm of insulating layer (SU-8). Prior to use, gold chips were cleaned by 5 min sonication in acetone (Sigma Aldrich, USA, no. 650501) followed by isopropanol (Sigma Aldrich, USA, no. W292907). To ensure a clean surface, the chips were then treated with oxygen plasma using a Zepto Diener plasma cleaner (Diener Electronics, Germany) at 0.5 mbar and 50% power for 2 min.

Nanocomposite preparation and activation

Nanocomposite coating was prepared using the previously described method[25]. Briefly, amine-functional reduced graphene oxide (Sigma Aldrich, USA, no. 805432) was dissolved in 5 mg/mL BSA (Sigma Aldrich, USA, no. 05470) in 10 mM PBS solution, pH 7.4 (Sigma Aldrich, USA, no. D8537), and ultrasonicated for 1h using 1s on/off cycles at 50% power. The solution was then denatured by heating at 105 °C for 5 min and centrifuged to remove the excess aggregates. The nanomaterial solution was then crosslinked by mixing with 70% glutaraldehyde (Sigma Aldrich, USA, no. G7776) at a ratio of 69:1, deposited on the glass chip with the gold electrodes and incubated in a humidity chamber for 20-24h to form a conductive nanocomposite[26]. After nanocomposite deposition, gold chips were washed in PBS by agitation (500 rpm) for 10 min and dried with pressurized air. EDC (Thermo Fisher Scientific, USA, no. 22980) and NHS (Sigma Aldrich, USA, no.

130672) were dissolved in 50 mM MES buffer (pH 6.2) at 400 mM and 200 mM, respectively, and deposited on nanocomposite-covered gold chips for 30 min. After surface activation, chips were quickly rinsed with ultra-pure water and dried, and the capture probes were spotted on top of the working electrode area.

Clinical samples and ethics statement

De-identified clinical saliva samples from the Dominican Republic were obtained from Boca Biolistics under their ethical approvals. RT-qPCR was performed by Boca Biolistics using the Perkin Elmer New Coronavirus Nucleic Acid Detection kit. De-identified clinical plasma samples were obtained from the Crimson Biomaterials Collection Core Facility at Partners Healthcare (currently Mass General Brigham). Additional de-identified clinical plasma and saliva samples were obtained through the Massachusetts Consortium on Pathogen Readiness (MassCPR) and had been collected by Prof. Jonathan Li and Prof. Xu Yu. Additional pre-SARS-CoV-2 pandemic samples were obtained from the Walt Laboratory at Brigham and Women's Hospital. The Institutional Review Board at the MGH, MGB, and Harvard University as well as the Harvard Committee on Microbiological Safety approved the use of the clinical samples in this study.

All clinical samples were inactivated by heating at 65 °C for 30 min prior to use to denature SARS-CoV-2 virions that might be present in the samples. We extracted total RNA from saliva via a QIAamp viral RNA mini kit (Qiagen), following manufacturer's instructions and eluted the total RNA in nuclease-free water.

CRISPR-based assay

CRISPR-based assays require the selection of both LAMP isothermal amplification primers and gRNAs to detect the LAMP amplicons. LAMP amplification primers (Supplementary Table S3), were selected after testing a range of LAMP primers, including some from the literature[28-32]. Cas12a gRNAs consist of two parts: the handle region (UAAUUUCUACUAAGUGUAGAU) that the Cas protein recognizes and binds, and a user-defined region at the 3' end of the handle that determines the specificity to the target. Spacer regions were selected following established guidelines[18]. To synthesize the gRNA (gRNA sequence: UAA UUU CUA CUA AGU GUA GAU GGU GAA ACA UUU GTC ACG CA), synthetic DNA with an upstream T7 promoter sequence (5′ GAAATTAATACGACTCACTATAGGG 3′) was purchased from Integrated DNA Technologies (IDT) and in vitro transcribed using the HiScribe T7 High Yield RNA Synthesis kit from New England Biolabs (NEB). Reactions were incubated for 16 h at 37 °C, treated with DNase I (NEB), and purified using the RNA Clean & Concentrator-25 kit (ZymoResearch). gRNA was quantified (ng/μL) on a Nanodrop 2000 (Thermo Fisher Scientific).

Simulated SARS-CoV-2 samples were prepared by serially diluting full length SARS-CoV-2 viral RNA (Twist Biosciences, MT106054.1) in nuclease-free water. Viral RNA extracted from saliva samples was used after purification via the QiAmp viral RNA extraction kit, as explained above. RNA was then amplified by LAMP and further detected by collateral cleavage of the fluorophore-quenched ssDNA reporter probe. Briefly, 5 μL of the diluted genomic DNA, or clinical sample RNA extract was added to 2.5 μL of the 10X primer mix (Supplementary Table S3), 12.5 μL of the LAMP master mix (NEB), and 5 μL of water. LAMP mixtures were incubated for 30 min at 65 °C. After

LAMP amplification, 4 μL of the amplified LAMP mixture were mixed with 11 μL of nuclease-free water and 5 μL of the CRISPR mixture, which contained 1 μM ssDNA fluorophore-quencher reporter (sequence: 6-FAM/TTATT/IABkFQ), 100 nM Cas, 200 nM gRNA in 10X NEB 2.1 buffer. Reactions were incubated at 37 °C for 20 min and fluorescence kinetics were measured using a BioTek NEO HTS plate reader (BioTek Instruments) with readings every 2 min (excitation: 485 nm; emission 528 nm).

Chip functionalization for the electrochemical CRISPR-based assay

For CRISPR sensors, custom synthesized amine-terminated peptide nucleic acid (AEEA-ACAACAACAACAACA) where AEEA is an O-linker was obtained from PNAbio, USA. PNA is a synthetic analog of DNA with a backbone utilizing repeating units of N-(2-aminoethyl) glycine linked through amide bonds. PNA contains the same four nucleotide bases as DNA – adenine, cytosine, guanine, and thymine – but are connected through methylene bridges and a carbonyl group to the central amine of a peptide backbone[61]. Stock PNA was diluted to 20 μM in 50mM MES buffer and spotted on the working electrode. One electrode was spotted with 1 mg/mL BSA as a negative control. The spotted chips were incubated overnight in a humidity chamber. After conjugation, chips were washed and quenched in 1 M ethanolamine dissolved in 10 mM PBS, pH 7.4 for 30 min and blocked with 1% BSA in 10 mM PBS containing 0.05% Tween 20.

SARS-CoV-2 CRISPR-based electrochemistry assays

The reporter sequence for CRISPR-based electrochemical assays was a ssDNA (sequence: /5Biosg/AT TAT TAT TAT TAT TTG TTG TTG TTG TTG T) conjugated to a biotin that bound to poly-streptavidin-HRP. Upon Cas12a activation, the ssDNA-biotin reporter is cleaved in solution, thus preventing binding to the complementary PNA sequence on the surface. Poly-streptavidin-HRP is then added and able to bind to the ssDNA reporter-biotin. The concentration of HRP bound to the electrode was read by HRP-dependent oxidation of precipitating TMB (TMB enhanced one component, Sigma Aldrich, US, no. T9455). TMB precipitation forms an insulating, non-soluble layer on the electrode surface. Full-length genomic RNA (Twist Biosciences, MT106054.1) was serially diluted and amplified with 2X LAMP master mix (NEB) for 30 min at 65 °C. Viral RNA was extracted from saliva via purification with the QiAmp viral RNA extraction kit. Similar to the protocol explained above, 5 μL of the viral RNA was added to 2.5 μL of the 10X primer mix (Supplementary Table S3), 12.5 μL of the LAMP master mix (NEB), and 5 μL of water. LAMP mixtures were incubated for 30 min at 65 °C. After LAMP amplification, 4 μL of the amplified LAMP product was mixed with 10 μL of nuclease-free water and 5 μL of the CRISPR mix, which contained 4 nM reporter, 100 nM Cas, 200 nM gRNA in 10X NEB 2.1 buffer. Mixtures were incubated for 20 min at 37 °C, during which time the ssDNA biotinylated reporter was cleaved. After that, 15 μL of the LAMP/reporter/Cas mixtures were deposited on the chips for 5 min. Thereafter, the chips were washed and incubated with poly-HRP streptavidin and TMB for 5 min and 1 min, respectively. Final measurement was then performed in PBST using a potentiostat (Autolab PGSTAT128N, Metrohm; VSP, Bio-Logic) by a CV scan with 1 V/s scan rate between -0.5 and 0.5 V vs on-chip integrated gold quasi reference electrode. Peak oxidation current was calculated using Nova 1.11 software. Cyclic voltammetry allowed us to measure attomolar concentrations of SARS-CoV-2 target RNA.

Serology ELISA assay

ELISA assays were optimized in a 96-well plate format. 100 µL of 1 µg/mL antigens: Spike S1 (SinoBiological, China, no. 40591-V08H), Nucleocapsid (RayBiotech, US, no. 130-10760) and Spike (S1) RBD (The Native Antigen Company, UK, no. REC31849) were prepared in a 10 mM PBS buffer at pH 7.4 and added to Nunc™ MaxiSorp™ ELISA plates (BioLegend, no. 423501) and immobilized on the plates by overnight incubation at 4 °C. The plates were washed three times with 200 µL of PBST followed by the addition of 250 µL of 5% Blotto for 1 h. After washing the plates, 100 µL of the clinical plasma samples diluted in 2.5% Blotto were added and incubated for 1h at RT. Plates were further washed and HRP conjugated anti-human IgA/IgM or biotin-conjugated anti-human IgG detection antibodies were added for 1h. The secondary antibodies used were: HRP conjugated anti-human IgM (Human IgM mu chain rabbit Antibody, Rockland, us, no. 109-4107) or IgA (AffiniPure Goat Anti-Human Serum IgA, α chain specific, Jackson ImmunoResearch, US, no. 109-005-011) or biotin-anti-human IgG (AffiniPure Goat Anti-Rabbit IgG, Fc fragment specific, Jackson ImmunoResearch, US, no. 111-005-008). The IgG plate was further mixed with 100µL of Streptavidin-HRP (1:200 dilution in 2.5 % Blotto) and washed. 100 µL of turbo TMB (Thermo Scientific, no. 34022) was added for 20 min followed by the addition of 100 µL of sulfuric acid (0.1M H_2SO_4 in Water) to stop the reaction. The absorbance of the plates was immediately read using a microplate reader (BioTek NEO HTS plate reader, BioTek Instruments) at 450 nm.

Electrochemical serology assay

To translate the ELISA assays to electrochemical readouts, Spike S1, Nucleocapsid and Spike-RBD were diluted to 1 mg/mL in the PBS buffer and spotted in three electrodes of the EC chip. An additional electrode was spotted with 1 mg/mL BSA as a negative control. The spotted chips were incubated overnight in a humidity chamber. After conjugation, chips were washed and quenched in 1 M ethanolamine (Sigma aldrich, US, no.E9508) dissolved in 10 mM PBS, pH 7.4 for 30 min and blocked with 5% Blotto (Santa Cruz Biotechnology, US, no. sc-2324) in 10 mM PBS containing 0.05% Tween 20 (Sigma aldrich, US, no. P9416). The fabricated sensor was then used to detect immunoglobulins from clinical samples.

Each sensor was either used to detect IgG, IgM, or IgA against the three antigens that were immobilized on the chips. 1.5 µL of clinical plasma samples were mixed with 13.5 µL of 2.5% Blotto and incubated on the chips for 30 min at RT followed by a rinsing step. After that, HRP conjugated anti-human IgM /IgA/ biotin-anti-human IgG was added for 30 min at RT. 1 µg/mL of poly-HRP-streptavidin (ThermoScientific, US, no. N200) diluted in 0.1 % BSA in PBST was added to chips with IgG for 5 min. The chips were rinsed and precipitating TMB was added for 3 min followed by final rinse and electrochemical measurement using a potentiostat by cyclic voltammograms with a scan rate of 1 V/s between -0.5 and 0.5 V vs on-chip integrated gold quasi reference electrode. Additional antibodies were screened, including: F(ab')2 Goat anti-Human IgG-Fc Fragment Antibody Biotinylated (Bethyl Laboratories, no. A80-148B), Goat anti-Human IgG Fc Secondary Antibody, Biotin (ThermoFisher Scientific, US, no. A18821), Purified anti-human IgG Fc Antibody (BioLegend, no. 409302), Purified anti-human IgG Fc Antibody (BioLegend, no. 410701), and AffiniPure $F(ab')_2$ Fragment Goat Anti-Human IgG, Fcγ fragment specific-biotin (Jackson ImmunoResearch, US, no. 109-006-170).

Multiplexed electrochemical serology and CRISPR-based RNA detection

Multiplexed sensors for both nucleic acid and host antibody detection were prepared by spotting three electrodes of the EC chip with proteins: Spike S1, Nucleocapsid and Spike-RBD; and spotting the amine-terminated peptide nucleic acid (AEEA-ACAACAACAACAACA) reporter on the fourth electrode. The spotted chips were incubated overnight in a humidity chamber. After conjugation, chips were washed and quenched in 1 M ethanolamine (Sigma aldrich, US, no.E9508) dissolved in 10 mM PBS, pH 7.4 for 30 min and blocked with 1% BSA in 10 mM PBS containing 0.05% Tween 20 (Sigma Aldrich, US, no. P9416). The fabricated sensor was then used to detect IgG's as well as viral RNA from clinical samples.

Multiplexed chips were used to detect viral RNA as well as IgG against the three antigens that were immobilized on the chips. Negative control saliva (RT-qPCR negative) was heat-inactivated and spiked with plasma at a ratio of 1:20 to simulate IgG concentrations in saliva. Two experiments were done in parallel in each chip, as follows: (1) 15μl of plasma-spiked saliva were used for the serology assays as explained above. Briefly, 0.75 μl of the plasma sample were mixed with 14.25 μl of control saliva and incubated on the chips for 30 min at RT followed by a rinsing step. After that, biotin-anti-human IgG was added for 30 min at RT. Chips were then rinsed. (2) In parallel, RNA extracted from RT-qPCR positive and negative clinical samples was amplified by LAMP for 30min at 65ºC as explained above. Then, 4 μL of the amplified LAMP product was mixed the CRISPR mix, which contained the electrochemical biotinylated reporter and incubated for 20min at 37ºC. 15 μL of the LAMP/reporter/Cas mixtures were deposited on the chips after the chips had been exposed to SARS-CoV-2 IgG. Thereafter, the chips were washed and incubated with poly-HRP streptavidin and TMB for 1 min. Final measurement was then performed in PBST using a potentiostat (Autolab PGSTAT128N, Metrohm; VSP, Bio-Logic) by a CV scan with 1 V/s scan rate between -0.5 and 0.5 V vs on-chip integrated gold quasi reference electrode. Peak oxidation current was calculated using Nova 1.11 software. Cyclic voltammetry allowed us to measure both the presence of IgG antibodies as well as attomolar concentrations of SARS-CoV-2 target RNA.

Data analysis

Fluorescence values are reported as absolute values for all experiments used for CRISPR-based fluorescence assays. Absorbances for the ELISA assays are reported as background-subtracted values to normalize for plate-to-plate variability. Peak oxidation current for electrochemical CRISPR and serology assays was calculated using Nova 1.11 software. All data were plotted, and statistical tests were performed using GraphPad Prism 8. Gold standards for ROC curve analysis: the individual samples for both serology and viral RNA detection were validated using SARS-CoV-2 RT-qPCR. For molecular assays, SARS-CoV-2 positive saliva samples were RT-qPCR positive at the time of saliva collection. For serology assays, SARS-CoV-2 positive plasma samples were RT-qPCR positive at the time of plasma or at an earlier date. Receiver operating characteristic (ROC) curves were used to evaluate the performance of diagnostic assays as a function of the discrimination threshold, plotted as sensitivity (%) versus 100-specificity (%). The areas under the ROC curve (AUC) are a proxy of test performance, where 1 represents a perfect test and 0.5 represents a random predictor. ROC curve analysis was done in GraphPad Prism 8 using a 95% confidence interval and the Wilson/Brown method. Figures were created using PowerPoint, BioRender or Adobe Illustrator.

Data availability

All data needed to evaluate the conclusions of this work can be found in the paper and/or the Supplementary Materials.

References

1. Wolfel, R.*, et al.* Virological assessment of hospitalized patients with COVID-2019. *Nature* **581**, 465-469 (2020).
2. Pan, Y., Zhang, D.T., Yang, P., Poon, L.L.M. & Wang, Q.Y. Viral load of SARS-CoV-2 in clinical samples. *Lancet Infectious Diseases* **20**, 411-412 (2020).
3. Zou, L.R.*, et al.* SARS-CoV-2 Viral Load in Upper Respiratory Specimens of Infected Patients. *New England Journal of Medicine* **382**, 1177-1179 (2020).
4. Gudbjartsson, D.F.*, et al.* Humoral Immune Response to SARS-CoV-2 in Iceland. *New England Journal of Medicine* **383**, 1724-1734 (2020).
5. Gaebler, C.*, et al.* Evolution of antibody immunity to SARS-CoV-2. *Nature* **591**, 639-644 (2021).
6. Van Elslande, J.*, et al.* Antibody response against SARS-CoV-2 spike protein and nucleoprotein evaluated by four automated immunoassays and three ELISAs. *Clinical Microbiology and Infection* **26**(2020).
7. Dispinseri, S.*, et al.* Neutralizing antibody responses to SARS-CoV-2 in symptomatic COVID-19 is persistent and critical for survival. *Nature Communications* **12**, 2670 (2021).
8. Nilsson, A.C.*, et al.* Comparison of six commercially available SARS-CoV-2 antibody assays-Choice of assay depends on intended use. *International Journal of Infectious Diseases* **103**, 381-388 (2021).
9. Fenwick, C.*, et al.* Changes in SARS-CoV-2 Spike versus Nucleoprotein Antibody Responses Impact the Estimates of Infections in Population-Based Seroprevalence Studies. *Journal of Virology* **95**(2021).
10. Meyer, B., Drosten, C. & Muller, M.A. Serological assays for emerging coronaviruses: Challenges and pitfalls. *Virus Research* **194**, 175-183 (2014).
11. Gilbert, P.B.*, et al.* Immune Correlates Analysis of the mRNA-1273 COVID-19 Vaccine Efficacy Trial. *medRxiv*, 2021.2008.2009.21261290 (2021).
12. Chen, J.S.*, et al.* CRISPR-Cas12a target binding unleashes indiscriminate single-stranded DNase activity. *Science* **360**, 436-439 (2018).
13. Gootenberg, J.S.*, et al.* Nucleic acid detection with CRISPR-Cas13a/C2c2. *Science* **356**, 438-442 (2017).
14. Gootenberg, J.S.*, et al.* Multiplexed and portable nucleic acid detection platform with Cas13, Cas12a, and Csm6. *Science* **360**, 439-444 (2018).
15. Lee, R.A.*, et al.* Ultrasensitive CRISPR-based diagnostic for field-applicable detection of Plasmodium species in symptomatic and asymptomatic malaria. *Proceedings of the National Academy of Sciences of the United States of America* **117**, 25722-25731 (2020).
16. Kaminski, M.M.*, et al.* A CRISPR-based assay for the detection of opportunistic infections post-transplantation and for the monitoring of transplant rejection. *Nature Biomedical Engineering* **4**, 601-609 (2020).
17. English, M.A.*, et al.* Programmable CRISPR-responsive smart materials. *Science* **365**, 780-785 (2019).
18. Gayet, R.V.*, et al.* Creating CRISPR-responsive smart materials for diagnostics and programmable cargo release. *Nature Protocols* **15**, 3030-3063 (2020).
19. Xu, W., Jin, T., Dai, Y.F. & Liu, C.C. Surpassing the detection limit and accuracy of the electrochemical DNA sensor through the application of CRISPR Cas systems. *Biosensors & Bioelectronics* **155**, 112100 (2020).
20. Bruch, R.*, et al.* CRISPR/Cas13a-Powered Electrochemical Microfluidic Biosensor for Nucleic Acid Amplification-Free miRNA Diagnostics. *Advanced Materials* **31**, 1905311 (2019).

21. de Puig, H., Bosch, I., Collins, J.J. & Gehrke, L. Point-of-Care Devices to Detect Zika and Other Emerging Viruses. *Annual Review of Biomedical Engineering, Vol 22* **22**, 371-386 (2020).
22. Liu, R.*, et al.* Analysis of adjunctive serological detection to nucleic acid test for severe acute respiratory syndrome coronavirus 2 (SARS-CoV-2) infection diagnosis. *International Immunopharmacology* **86**(2020).
23. Torrente-Rodriguez, R.M.*, et al.* SARS-CoV-2 RapidPlex: A Graphene-Based Multiplexed Telemedicine Platform for Rapid and Low-Cost COVID-19 Diagnosis and Monitoring. *Matter* **3**(2020).
24. Yuan, Q.L.*, et al.* Highly stable and regenerative graphene-diamond hybrid electrochemical biosensor for fouling target dopamine detection. *Biosensors & Bioelectronics* **111**, 117-123 (2018).
25. Zupancic, U., Jolly, P., Estrela, P., Moschou, D. & Ingber, D.E. Graphene Enabled Low-Noise Surface Chemistry for Multiplexed Sepsis Biomarker Detection in Whole Blood. *Advanced Functional Materials* **31**(2021).
26. del Rio, J.S., Henry, O.Y.F., Jolly, P. & Ingber, D.E. An antifouling coating that enables affinity-based electrochemical biosensing in complex biological fluids. *Nature Nanotechnology* **14**, 1143-1149 (2019).
27. Timilsina, S.S.*, et al.* Rapid antifouling nanocomposite coating enables highly sensitive multiplexed electrochemical detection of myocardial infarction and concussion markers. *medRxiv*, 2021.2006.2013.21258856 (2021).
28. Rabe, B.A. & Cepko, C. SARS-CoV-2 detection using isothermal amplification and a rapid, inexpensive protocol for sample inactivation and purification. *Proceedings of the National Academy of Sciences of the United States of America* **117**, 24450-24458 (2020).
29. Lu, R.F.*, et al.* Development of a Novel Reverse Transcription Loop-Mediated Isothermal Amplification Method for Rapid Detection of SARS-CoV-2 (vol 18, pg 615, 2020). *Virologica Sinica* **35**, 499-499 (2020).
30. Rohaim, M.A.*, et al.* Artificial Intelligence-Assisted Loop Mediated Isothermal Amplification (AI-LAMP) for Rapid Detection of SARS-CoV-2. *Viruses-Basel* **12**(2020).
31. Nawattanapaiboon, K.*, et al.* Colorimetric reverse transcription loop-mediated isothermal amplification (RT-LAMP) as a visual diagnostic platform for the detection of the emerging coronavirus SARS-CoV-2. *Analyst* **146**, 471-477 (2021).
32. Yan, C.*, et al.* Rapid and visual detection of 2019 novel coronavirus (SARS-CoV-2) by a reverse transcription loop-mediated isothermal amplification assay. *Clinical Microbiology and Infection* **26**, 773-779 (2020).
33. FDA. CDC 2019-nCoV Real-Time RT-PCR Diagnostic Panel (CDC) - Manufacturer Instructions/Package Insert I FDA, (available at https://www.fda.gov/media/134922/download).
34. Ter-Ovanesyan, D.*, et al.* Ultrasensitive Measurement of Both SARS-CoV-2 RNA and Antibodies from Saliva. *Analytical Chemistry* **93**, 5365-5370 (2021).
35. Satarker, S. & Nampoothiri, M. Structural Proteins in Severe Acute Respiratory Syndrome Coronavirus-2. *Archives of Medical Research* **51**, 482-491 (2020).
36. Huang, Y., Yang, C., Xu, X.F., Xu, W. & Liu, S.W. Structural and functional properties of SARS-CoV-2 spike protein: potential antivirus drug development for COVID-19. *Acta Pharmacologica Sinica* **41**, 1141-1149 (2020).
37. Hou, H.Y.*, et al.* Detection of IgM and IgG antibodies in patients with coronavirus disease 2019. *Clinical & Translational Immunology* **9**(2020).
38. Grossberg, A.N.*, et al.* A multiplex chemiluminescent immunoassay for serological profiling of COVID-19-positive symptomatic and asymptomatic patients. *Nature Communications* **12**(2021).

39. Sterlin, D.*, et al.* IgA dominates the early neutralizing antibody response to SARS-CoV-2. *Science Translational Medicine* **13**(2021).
40. Isho, B.*, et al.* Persistence of serum and saliva antibody responses to SARS-CoV-2 spike antigens in COVID-19 patients. *Science Immunology* **5**, eabe5511 (2020).
41. Zohar, T.*, et al.* Compromised Humoral Functional Evolution Tracks with SARS-CoV-2 Mortality. *Cell* **183**, 1508-1519 (2020).
42. Yurkovetskiy, L.*, et al.* Structural and Functional Analysis of the D614G SARS-CoV-2 Spike Protein Variant. *Cell* **183**, 739-751 (2020).
43. Calistri, P.*, et al.* Infection sustained by lineage B.1.1.7 of SARS-CoV-2 is characterised by longer persistence and higher viral RNA loads in nasopharyngeal swabs. *International Journal of Infectious Diseases* **105**, 753-755 (2021).
44. Fajnzylber, J.*, et al.* SARS-CoV-2 viral load is associated with increased disease severity and mortality. *Nature Communications* **11**(2020).
45. van Kampen, J.J.A.*, et al.* Duration and key determinants of infectious virus shedding in hospitalized patients with coronavirus disease-2019 (COVID-19). *Nature Communications* **12**, 267 (2021).
46. Golubchik, T.*, et al.* Early analysis of a potential link between viral load and the N501Y mutation in the SARS-COV-2 spike protein. *medRxiv*, 2021.2001.2012.20249080 (2021).
47. Dörschug, A.*, et al.* Comparative Assessment of Sera from Individuals after S-Gene RNA-Based SARS-CoV-2 Vaccination with Spike-Protein-Based and Nucleocapsid-Based Serological Assays. *Diagnostics (Basel)* **11**(2021).
48. Ndaye, A.N., Hoxha, A. & Madinga, J. Challenges in interpreting SARS-CoV-2 serological results in African countries (vol 9, pg E588, 2021). *Lancet Global Health* **9**, E597-E597 (2021).
49. Schaffer DeRoo, S., Pudalov, N.J. & Fu, L.Y. Planning for a COVID-19 Vaccination Program. *Jama-Journal of the American Medical Association* **323**, 2458-2459 (2020).
50. Morshed, M.*, et al.* Comparative Analysis of Capillary vs Venous Blood for Serologic Detection of SARS-CoV-2 Antibodies by RPOC Lateral Flow Tests. *Open Forum Infectious Diseases* **8**(2021).
51. Prazuck, T.*, et al.* Evaluation of performance of two SARS-CoV-2 Rapid whole-blood finger-stick IgM-IgG Combined Antibody Tests. *medRxiv*, 2020.2005.2027.20112888 (2020).
52. Premkumar, L.*, et al.* The receptor-binding domain of the viral spike protein is an immunodominant and highly specific target of antibodies in SARS-CoV-2 patients. *Science Immunology* **5**(2020).
53. Nguyen, P.Q.*, et al.* Wearable materials with embedded synthetic biology sensors for biomolecule detection. *Nature Biotechnology* (2021).
54. de Puig, H.*, et al.* Minimally instrumented SHERLOCK (miSHERLOCK) for CRISPR-based point-of-care diagnosis of SARS-CoV-2 and emerging variants. *Science Advances* **7**, eabh2944 (2021).
55. Broughton, J.P.*, et al.* CRISPR-Cas12-based detection of SARS-CoV-2. *Nature Biotechnology* **38**, 870-874 (2020).
56. Rauch, J.N.*, et al.* A Scalable, Easy-to-Deploy Protocol for Cas13-Based Detection of SARS-CoV-2 Genetic Material. *Journal of Clinical Microbiology* **59**(2021).
57. Arizti-Sanz, J.*, et al.* Streamlined inactivation, amplification, and Cas13-based detection of SARS-CoV-2. *Nature Communications* **11**(2020).
58. Lee, R.A., Herigon, J.C., Benedetti, A., Pollock, N.R. & Denkinger, C.M. Performance of Saliva, Oropharyngeal Swabs, and Nasal Swabs for SARS-CoV-2 Molecular Detection: a Systematic Review and Meta-analysis. *Journal of Clinical Microbiology* **59**(2021).
59. Wyllie, A.L.*, et al.* Saliva or Nasopharyngeal Swab Specimens for Detection of SARS-CoV-2. *New England Journal of Medicine* **383**, 1283-1286 (2020).

60. Isho, B.*, et al.* Persistence of serum and saliva antibody responses to SARS-CoV-2 spike antigens in COVID-19 patients. *Science Immunology* **5**(2020).
61. Jolly, P., Rainbow, J., Regoutz, A., Estrela, P. & Moschou, D. A PNA-based Lab-on-PCB diagnostic platform for rapid and high sensitivity DNA quantification. *Biosensors & Bioelectronics* **123**, 244-250 (2019).
62. Long, Q.X.*, et al.* Antibody responses to SARS-CoV-2 in patients with COVID-19. *Nature Medicine* **26**, 845-848 (2020).

Acknowledgements

We would like to thank Tal Gilboa Hitron, Rose A. Lee and Nicole Weckman for helpful discussions and advice. This work was supported by the Wyss Institute for Biologically Inspired Engineering at Harvard University and the Paul G. Allen Frontiers Group. J.R. was funded through the UK Natural Environment Research Council (NERC) GW4 FRESH CDT. H.D.P. was supported by the Harvard University Center for AIDS Research (CFAR), an NIH-funded program (P30 AI060354), which is supported by the following NIH co-funding and participating Institutes and Centers: NIAID, NCI, NICHD, NIDCR, NHLBI, NIDA, NIMH, NIA, NIDDK, NINR, NIMHD, FIC, and OAR. The MGH/MassCPR COVID biorepository was supported by a gift from Ms. Enid Schwartz, by the Mark and Lisa Schwartz Foundation, the Massachusetts Consortium for Pathogen Readiness and the Ragon Institute of MGH, MIT and Harvard.

Author contributions

HDP and PJ formulated the idea, organized the experiments and contributed in project management. HDP, SS, JR and PJ conceived the study under the guidance of PE, JJC and DEI. Experiments were performed and validated by HDP, SS, JR, PJ, DN and ND. DRW, GA, JZL, XGY contributed in the collection and characterization of clinical serum and saliva samples. All authors contributed to manuscript preparation and editing.

Competing interests

HDP, PJ, JJC, DEI are inventors in patents describing the CRISPR electronics technology. PJ and DEI are listed as inventors on patents describing the electrochemical sensor platform. JJC and DRW are cofounders and directors of Sherlock Biosciences. All other authors declare no competing interests.